

# A compact, low-distortion imaging spectrometer for remote sensing

Pantazis Mouroulis and David A. Thomas  
Jet Propulsion Laboratory  
California Institute of Technology  
4800 Oak Grove Drive, Pasadena, CA 91109

## Abstract

We describe a pushbroom imaging spectrometer having a number of attractive features for remote sensing applications, including compact and simple form, good image quality, high efficiency, and very low levels of distortion. These properties are made possible by the unique characteristics of convex gratings manufactured by electron-beam lithography. A laboratory prototype has been built and is under evaluation. It has an f-number of 2.8, covers a spectral band from 400 to 1000 nm with 3 nm spectral resolution and has 750 spatial elements across the entrance slit. Experimental results are shown that demonstrate very low distortion, on the level of 2% of a pixel.

## 1. Introduction

Pushbroom imaging spectrometers are a desirable form for Earth observations from space, since they can achieve a higher signal-to-noise (s/n) ratio than their whiskbroom counterparts. At the same time, they carry the penalty of increased calibration difficulty. While in a whiskbroom spectrometer all pixels have their spectra recorded by the same one linear photodetector array, for a pushbroom spectrometer with 700-1000 spatial pixels there are effectively that many different linear arrays or spectrometers in need of calibration.

It has been recently recognized that the required calibration accuracy must be very high. The spectral response function (SRF) of a pixel must be known accurately. The desired uncertainty in the location of the peak of this function is on the order of 1% (e.g. 0.1 nm in 10 nm pixel bandwidth) in order to produce data that are free of significant spectral calibration errors. A similar tight tolerance applies to the variation of the halfwidth of the SRF.<sup>1</sup>

Translation of these tight calibration requirements to a pushbroom imaging spectrometer leads to a very difficult calibration task if there is any substantial variation of the SRF along the spatial direction. It is thus desirable to reduce such variation to very small levels. There are two consequences for the optical design: 1) the distortion must be controlled to a small fraction of a pixel, and 2) the point spread function (PSF) variation across the field must be small.

We distinguish two errors associated with distortion along the spatial and spectral directions. The first one is that the monochromatic slit image may be curved rather than straight. This is referred to as 'smile', and it is the error associated with the location of the peak of the SRF. The second error, called 'keystone', refers to the fact that the spectrum of any one point on the slit must be parallel to the spectrum of another point. This error does not enter directly into the spectral calibration of a pixel, but it causes mixing of the spectra from adjacent pixels. Though some level of this mixing is unavoidable, the presence of keystone means that the level of mixing varies with spatial location, thus complicating the extraction of information for any one pixel.

In this paper we are concerned primarily with demonstrating low levels of smile and the associated reduction in spectral calibration error. The current state of the art in pushbroom imaging spectrometers has reduced the above distortion errors down to approximately the quarter pixel level (25%), with some (as yet untested) designs claiming levels of about 10% in theory. In this paper, we demonstrate a laboratory prototype which approaches the 2% level, and has the potential for even further reduction. To our knowledge, this is the first time that a system is demonstrated to achieve these low levels of error.

## 2. The Offner spectrometer

The above requirements can be satisfied using what has come to be known as the Offner spectrometer form.<sup>2,3</sup> This relies on the Offner unity magnification reflective relay, which comprises two spherical concentric reflectors (concave and convex) with the convex one having half the radius of the concave. The following are the advantages of the Offner spectrometer form with a convex grating as dispersive element.

- It can operate at relatively low f-number (greater than about  $f/2$ ).
- It accepts a long slit while maintaining a highly compact form. Several useful designs have been produced in which the maximum spectrometer dimension is only four to five times the slit length. Since the design is scalable, an absolute slit length specification is not particularly meaningful. However, designs with 25-27mm slit length have been produced, which make use of the maximum possible dimension in IR detector arrays.
- It offers the potential for very small distortion in both spectral and spatial directions if appropriately optimized.
- It has only three (two) optical surfaces (excluding fold mirrors not fundamental to the design form).
- It typically utilizes only spherical and centered surfaces. This feature, in addition to ease of fabrication, provides the best possible chance of approximating the theoretical performance in practice.

Several compact Offner spectrometer designs have been produced spanning the ultraviolet to thermal IR spectral range, while presenting minimum smile and keystone errors, of approximately 1%. These designs are described in ref. 4.

Spectrometer forms based on the Offner relay have been proposed using curved prisms as the dispersing elements.<sup>5</sup> However, the addition of three curved prisms is a considerable complication. A grating-based design is simpler, provided the gratings can be of sufficient quality and of high enough efficiency. These requirements can be satisfied using gratings made by electron-beam lithography.

## 3. E-beam grating characteristics

The properties of convex gratings manufactured by E-beam lithography have been detailed elsewhere.<sup>6</sup> We give here a summary of the relevant characteristics.

The grating relief pattern is formed on a thin ( $\sim 2 \mu\text{m}$ ) layer of PMMA which is spun-coated onto the curved substrate. A reflective Al layer (30 – 50 nm thick) is evaporated on top. Adhesion, thermal cycling, vibration, and outgassing tests have been successfully performed as part of flight qualification.

These gratings can achieve the maximum possible efficiency under any desired spectral response specification. This is because the E-beam technique affords the flexibility of either varying the blaze angle or of keeping it constant across the extent of the grating. Typically, a blazed grating has the highest possible peak efficiency, but may not be adequate at short or at long wavelengths, depending on the width of the desired band. By varying the blaze angle, a broader band can be covered at the expense of peak efficiency. Since the E-beam technique generates the blaze angle of each groove independently by varying the exposure, it is possible to tailor the blaze angle variation to achieve a desired grating spectral response. In addition, coherence can be maintained from one groove to the next or from one panel to the next, unlike ruled gratings which normally show random or uncontrolled phase shifts between panels or areas with different blaze angles. A relative peak efficiency of around 88% in the first order has been consistently achieved for a single-blaze grating or grating panel. In addition to maximizing efficiency, the E-beam technique affords flexibility in constructing aberration-correcting gratings, or gratings with profiles that differ from the blazed sawtooth type for the purpose of obtaining a specified response.

E-beam gratings have been compared with holographic and ruled gratings of the same specifications, and have outperformed these other types not only in terms of diffraction efficiency, but also wavefront quality and scatter. Further, in terms of achieving the design values of smile and keystone, there are two critical characteristics of these gratings, which cannot be achieved through ruling techniques. These are 1) that the

phase shift between panels or different blaze areas is controllable, and 2) that the blaze areas (if more than one) can be made concentric, which minimizes the impact of intensity apodization on the location of the centroid of the PSF and hence on distortion.

#### 4. Description of the prototype spectrometer

The present device has the following characteristics: spectral range 400-1000nm with nominal 3 nm resolution per pixel (188 spectral pixels),  $f/2.8$ , and 750 spatial pixels. Though the optical design can support a greater number of spatial pixels, the limit is provided in this case by the photodetector array (CIDTEC 3710D). This is a nominal 754x484 CID array, with  $12 \times 13.7 \mu\text{m}$  pixels. Thus the maximum recorded slit length is 9 mm. The 400-1000 nm spectrum is recorded over only ~188 out of the 484 spectral pixels, but the extended image can be used to record also the 0<sup>th</sup> order, thus providing an easy means of wavelength calibration. The array has a fill factor of about 85%, the inactive area being occupied by a ~2  $\mu\text{m}$  Al strip running down the length of a column (along the long direction).

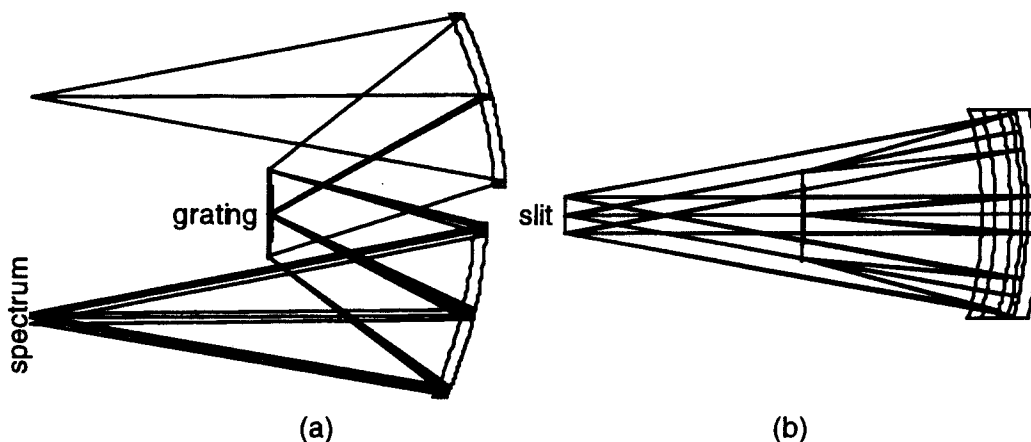
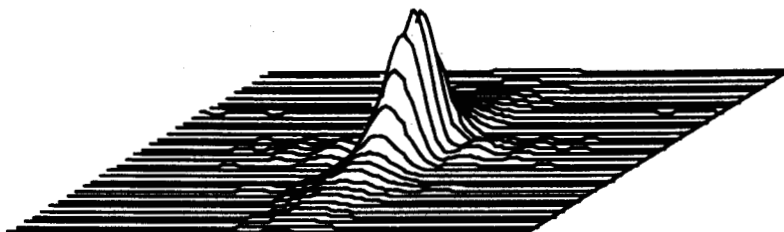


Figure 1. Prototype spectrometer schematic. The scale is approximately 0.5.

The optical design schematic is shown in figure 1. Though it might have been possible to design an even more compact form, the purpose of this prototype was to show that very low smile and keystone values can be achieved in practice, and to develop the necessary alignment and measurement techniques. Tolerance analysis revealed that two of the three curvatures could be fitted to manufacturer's testplates. The curvature of the tertiary, together with the spacings were then used as variables to re-optimize performance. The result of this process was an increase in the design values of smile from practically zero to about 2%, and of keystone to about 1.2%. Both these values were considered within tolerance for this demonstration. The tolerance on the tertiary radius of curvature was set at 0.1%. Other mirrors were toleranced at two fringes power and 0.5 fringe irregularity.

The design has essentially diffraction-limited performance at the long wavelength end (Strehl ratio  $>0.83$ ), while the ensquared energy within a pixel is about 92%. At the short wavelength end, where the diffraction spread is small, the ensquared energy is even higher, more than 96%, even though the image quality is somewhat degraded. The worst-case point spread function (PSF) is shown in figure 2. This is obtained at 400 nm and at the middle of the slit. It can be seen from figure 2 that the optical PSF is essentially fully contained in the pixel.



**Figure 2.** Worst-case PSF for the prototype spectrometer design. The size of the rectangle is approximately one pixel ( $13\ \mu\text{m}$ ). The Strehl ratio for this PSF is  $\sim 0.42$ .

Finally, another way to appreciate the image quality is through the system MTF, shown in figure 3. Again, the worst-case MTF only is shown, and it can be seen that the residual aberration has a rather small effect.

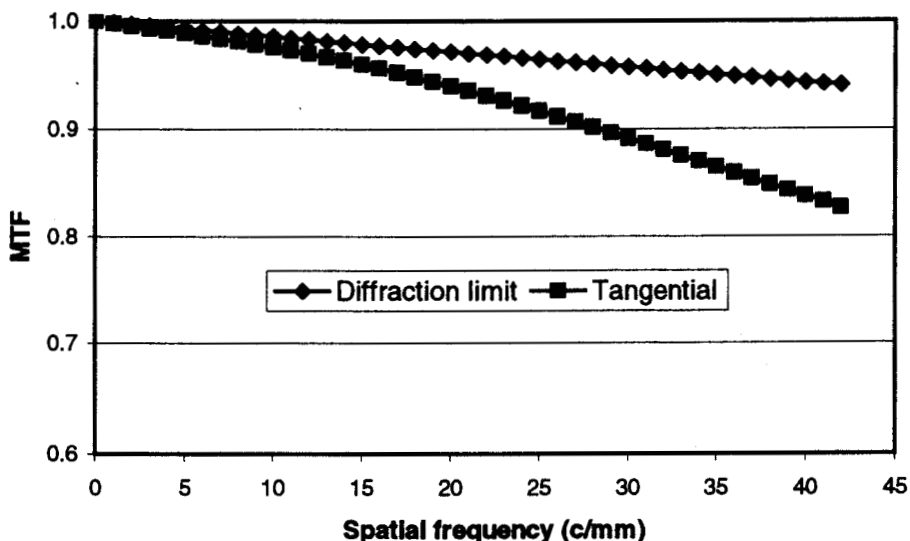


**Figure 3.** Worst-case design MTF for the prototype spectrometer. The maximum frequency shown corresponds to the Nyquist limit as determined by the detector pixel size.

The grating used for this spectrometer operated in the first order and did not have any partitions (panels), which gives optimum wavefront quality. The blaze angle remained constant relative to the local surface normal, thus providing true blazed grating behavior despite the substrate curvature. Further details of the performance of E-beam gratings are given in ref. 6.

## 5. Alignment

The spectrometer was assembled using standard optical laboratory mounts. The mirrors and grating were placed on x-y-z stages. In addition, the grating could be rotated on a goniometric stage in order to orient the grooves along the vertical direction with sufficient accuracy. The camera was placed on a mount with three degrees of freedom in translation as well as rotation.

The first task was to align the primary and tertiary to their common center of curvature. This was done by using an interferometer that illuminated both mirrors, and manually approaching the zero fringe condition for both mirrors simultaneously. This is a simple adjustment, typically accomplished in tens of minutes.

The spectrometer was then translated laterally so that the focus of the interferometer beam was placed at the center of the slit location. With the primary and tertiary thus fixed, the grating was then put in place by obtaining several interferograms of the complete spectrometer in double pass. It was found possible to approximate the theoretical performance within two to three hours of adjustment. The optical design software (ZEMAX) generated interferograms that showed  $0.8 \lambda$  p-v of astigmatism for a point object at the center of the slit and 632.8 nm wavelength. The actual value measured after adjustment was  $\sim 0.8 \lambda$  p-v of total wavefront error, with the following Seidel terms:  $0.5 \lambda$  of astigmatism,  $0.3 \lambda$  of spherical and  $0.2 \lambda$  of coma. The residual spherical and coma terms are probably a result of mirror surface quality. The fact that the amount of astigmatism is less than the design value implies that the spectrometer was not aligned at exactly the design condition, which, in any case would have been hard to achieve interferometrically. This alignment method accuracy was thought of as sufficient for a start. The optical design model confirmed that the level of smile was not affected by such a small residual misalignment.

## 6. Results

The smile was measured by using a  $28 \mu\text{m}$  wide slit at the input, illuminated by various spectral lamps. The slit was made through lithographic techniques for maximum accuracy and edge quality. The wavelengths tested were 435 nm (Hg), 546 nm (Hg), 760 nm (Kr), and 912 nm (Ar). Figure 4 shows a representative result obtained for the 546.1 nm Hg line. The figure shows two interpolated curves, linear and quadratic. The linear one represents residual misalignment between the camera and the slit, which can be seen to be at the 2% pixel level. The difference between the two interpolated curves represents the smile inherent in the sensor. It can be seen that this difference is again  $\sim 2\%$  of a pixel. Similar results were obtained with the other spectral lines. The 546 nm line gave the highest smile value.

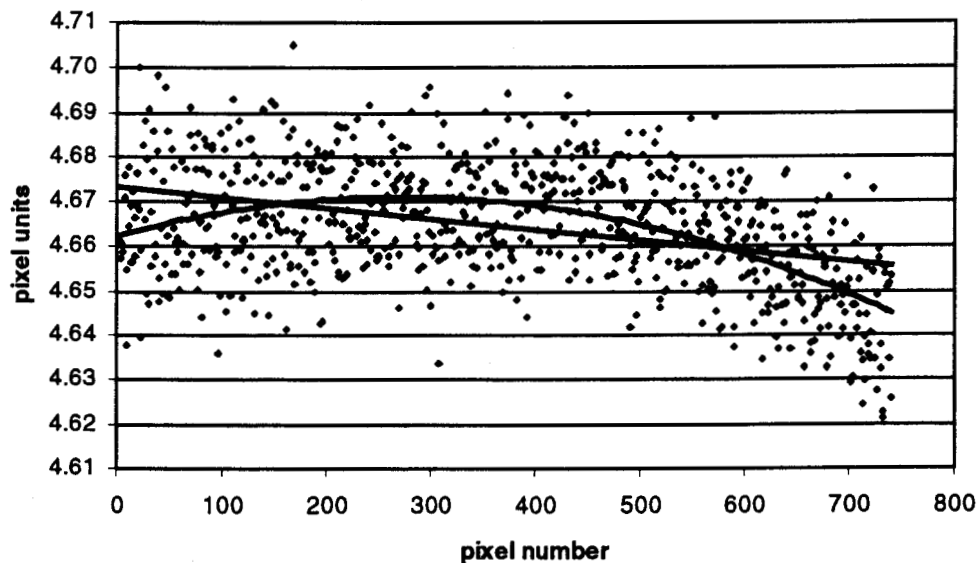


**Figure 4.** Image of the Hg 546.1 spectral line as obtained with the prototype spectrometer. Each point represents the centroid of approximately ten pixels along a column of the array. The horizontal axis gives the column (pixel) number.

In a real sensor, it would be desirable to minimize not only the smile but also the rotation of the focal plane shown in figure 4. This adjustment would require a more precise rotation stage than the one used for this preliminary experiment.

The simple centroiding calculation used to produce figure 4 assumes that the pixel response (or sensitivity) is uniform at the subpixel level. This is an assumption in need of closer examination, if one is to measure very low values of smile reliably. The detailed mapping of the pixel sensitivity<sup>7</sup> is a laborious process that was not undertaken here, but may be necessary if one seeks the ultimate accuracy and repeatability from these measurements.

The data of figure 4 represent an average of four frames. A larger number of frames tends to reduce the scatter but does not lead to a different shape of the interpolated lines. The errors associated with the measurement are more critically due to the influence of the slit illumination (which must be uniform) and the number of pixels that are averaged on either side of the spectral line. This number may be limited in practice by the presence of adjacent spectral lines. The influence of these factors leads us to estimate the accuracy of the current measurement technique to be similar to the level of smile demonstrated by the sensor.

In addition to low smile, the SRF halfwidth variation must remain small. At the time of writing no careful measurements of the SRF variation had been performed. However it is possible to obtain a general idea of what to expect from this spectrometer by using a simple theoretical simulation that simplifies the sub-pixel sensitivity response to a rect function, and also by using the computed diffraction PSF. The maximum SRF variation occurs at the shortest wavelength, where the image quality varies the most. This is shown in figure 5. This variation is quite small because the main lobe of the PSF is still considerably smaller than the pixel for any field location. Thus, although this spectrometer was not specifically optimized to show minimum SRF variation, it should still perform very well in that area. We may note however, that this is in a sense only half a spectrometer in terms of typical spectral coverage for Earth observations. The addition of another module to cover the band 1000-2500 nm would change this design by necessitating a longer slit, since this small pixel size cannot be maintained at longer wavelengths. The achievement of the same performance over the broader spectral band will then pose additional problems, especially if a very compact size is desired. However, the requirement for a longer slit is somewhat balanced by the larger pixel size which permits a greater PSF variation, as well as larger absolute values of smile and keystone. The spectrometer form presented here, with the possible incorporation of an aberration-balancing phase function at the grating, should still be capable of providing excellent performance.

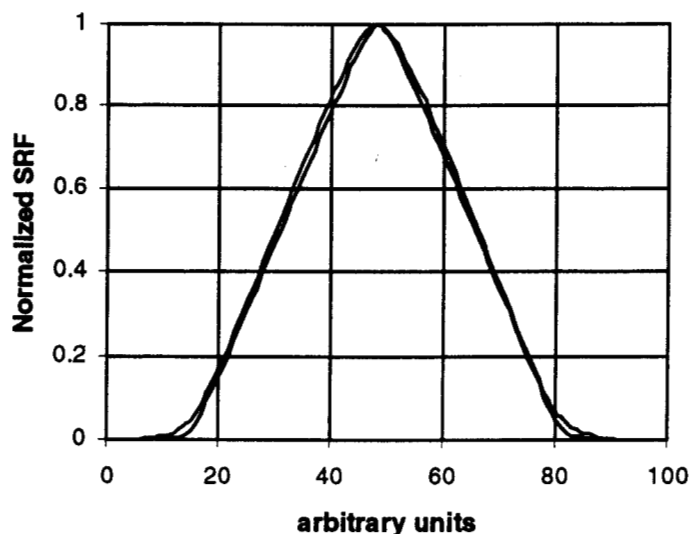


**Figure 5.** Maximum predicted SRF variation for the prototype spectrometer. The wider curve is the SRF arising from the PSF shown in figure 2. The narrower curve is the SRF from the corresponding best PSF (for a different field position) for the 400 nm wavelength.

## 7. Conclusions and outlook

This work has demonstrated a compact pushbroom imaging spectrometer module that can achieve very low values of smile in practice. The importance of low smile is that it reduces considerably the calibration difficulty of a pushbroom imaging spectrometer, because it implies that the center wavelength of the pixel SRF does not have to be measured except for one or two complete columns. The prototype design also exhibits very small SRF bandwidth variation across the field.

Work on this prototype spectrometer has only just begun. Future improvements in data gathering involve automatic averaging of a large number of frames, including frames that are shifted by a few microns at a time relative to each other. This is expected to improve the accuracy and repeatability of the measurements to the point where a 1% smile should be detectable reliably. The SRF variation must also be measured and compared with the design values. Finally, the level of keystone error must be ascertained, which is expected to be a more complicated measurement than that of smile.

## Acknowledgments

This research was performed at the Jet Propulsion Laboratory, California Institute of Technology, under a contract with the National Aeronautics and Space Administration. We thank Paul Maker, Dan Wilson, and Rich Muller of the JPL Microdevices Laboratory for providing us with the grating used in this prototype, and Mike McKerns (U. of Alabama, Birmingham) for technical assistance. We also wish to thank Jeff Simmonds, Barbara Wilson and Gregg Vane for their support of this project.

## References

1. R. O. Green, "Spectral calibration requirement for Earth-looking imaging spectrometers in the solar-reflected spectrum", *Appl. Opt.* **37**, 683-690 (1998).
2. A. Offner: "Unit power imaging catoptric anastigmat", U.S. Patent No. 3,748,015 (1973)
3. L. Mertz: "Concentric spectrographs", *Appl. Opt.* **16**, 3122-3124 (1977)
4. P. Mouroulis: "Low-distortion imaging spectrometer designs utilizing convex gratings", 1998 International Optical Design Conference (to appear as SPIE vol. 3482).
5. D. R. Lobb: "Imaging spectrometers using concentric optics" in *Imaging Spectrometry III*, Proc. SPIE **3118**, 339-347 (1997).
6. P. Mouroulis, D. W. Wilson, P. D. Maker, and R. E. Muller: "New convex grating types for concentric imaging spectrometers", *Applied Optics* (in press).
7. D. Kavaldjiev and Z. Ninkov: "Subpixel sensitivity map for a charge-coupled device sensor", *Opt. Eng.* **37**, 948-954 (1998).